preprint version from June 06. 2021

A Rapid Design Approach for Transverse Flux Machines in Underwater Applications

Christoph Stoeffler[1*], Michael Zipper[2] and Jonathan Babel[1]

[1]AG Robotik, Universität Bremen, Germany
(stoeffle@uni-bremen.de)* Corresponding author
(jonathan.babel@dfki.de)
[2]German Research Center for Artificial Intelligence, Bremen, Germany
(michael.zipper@dfki.de)

Abstract: In this work, we show a design procedure for *Transverse Flux Machines* that belong to the class of *direct drives*, which become more relevant in robotics - also for underwater applications. These drives exhibit a range of advantages, due to the omittance of gears. This usually requires that the geometry is adapted to the motor's use case, which is a demanding task. An analytical modeling approach, based on the work of Pourmoosa [14], is used in combination with the open-source software *OpenModelica* to simulate arbitrary designs of this type. This allows a fast simulation of a multitude of motors. In combination with a specifically constructed genetic algorithm, we show that preferable designs can be obtained under predefined performance parameters. The method therefore gives rise to useful pre-computations for drives of this kind and potentially allows their usage in more robotic applications.

Keywords: Sensors and Actuators

1. INTRODUCTION

The demand for robotic systems with increased performance is becoming more relevant these days in order to bring them to new levels of application. Such amendments include - among others - high robustness, simpler designs and dynamic behaviour. This can hardly be achieved by advanced algorithms alone and requires new approaches in the design and manufacturing of hardware on an elementary level. Brushless DC motors in combination with high reduction gears are common solutions for joint actuation within robotic systems, as they allow sufficiently accurate control paired with high energy efficiency. Asada and Kanade [1] already suggested a direct drive for robotic applications, arguing that heavy transmission gears and large friction and backlash in classical drives prevent dynamic and fine movements. For the same reasons the design of *Transverse Flux Machines* (TFMs) has been pursued in [4]. Seok and others [6] show in contrast that it is reduced *apparent inertia* (or *reflected inertia* - see [11]) and higher control bandwidth what makes direct-drives preferable for dynamic applications. For underwater robots, direct-drives have long been used to power propellers and impellers. The simplicity in design is a major advantage of these drives, as outlined e.g. by [2]. In [7] it is however reported that one drawback of electric DC motors is the high revolutionary speed which is often beyond the intended speed of propellers. The current paradigm shift in underwater locomotion towards drives with a high torque-to-weight ratio leverages soft robotic actuators with sufficient large amplitudes at lower speeds. Current soft robotic systems with high efficiency, still rely on classical electromagnetic drives, as shown e.g. by [13]. Moreover, new measurement possibilities for underwater applications arise with direct drives, due to a more reliable torque measurement, leading to designs beyond the ones described in [9]. Our goal is therefore to develop a specific tailored underwater drive aiming at both, high efficiency and simplicity. TFMs achieve high torque densities - see e.g. [12] with a distinct layout. The flux path is transverse to the direction of movement allowing the decoupling of the magnetic and electric circuits. A major drawback of TFMs is their low power factor due to high flux leakages along with high *cogging torque*[1]. Researchers are striving to overcome these problems with designs that deviate from the simple TFM geometry, given in Fig. 1. Accordingly, different classifications of TFMs exist in the literature, like seen e.g. in [12] and [10, p. 91]. This work proposes a strategy to quickly obtain motor geometries of TFMs that can be used for further development phases (e.g. "warm start" of detailed simulations) of these drives. In Section 2, analytical modeling approaches for TFMs are being discussed. Moreover, a genetic algorithm is introduced, which iterates through many motor designs and

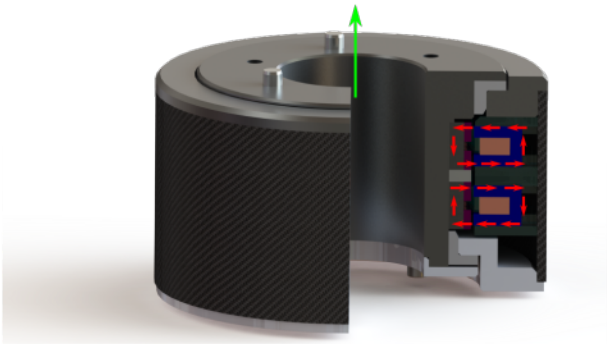

Fig. 1. Design of a two-phase TFM - green: rotation axis, red: magnetic flux in transverse planes

[1]The jerkiness of a drive due to its magnets interacting with the stator slots

ensures to work in a wide parameter range, but requires fast simulations, as they are given from analytical models. The entire procedure for deriving an optimized motor design is presented in Section 3and concluded in the final discussion in Section 4.

2. ANALYTICAL MODELING OF TRANSVERSE FLUX MACHINES

Whereas *Finite Element Methods* (FEM) solve the entirety of *Maxwell's equations* over the domain of the motor geometry, analytical methods generally approximate the solution in one way or another. Often, only a local solution of the quasi-static formulation of Maxwell's equation is given. A good overview of analytical modeling approaches on TFM's is given in [10]. It must be noted that the hereafter described method can only serve for a first iteration in the motor design procedure, since modeling assumptions and reasonable separation of flux paths can lead to comparable high errors up to 30 %, depending on motor position (see [10]). Compared to FEM, analytical methods are generally less accurate, but much faster in computational time. However, analytical models in combination with genetic algorithms allow to sample through a sufficient big parameter space, being more likely to reveal a global optimum in design.

2.1 Magnetic Equivalent Circuits

The idea behind *Magnetic Equivalent Circuits* (MEC) is to treat the magnetic flux appearing in magnetically conductive materials (or vacuum) in analogy to electric current in electrically conductive material - see e.g. [3, p.97]. Generally, in quasi-static formulation, the integral

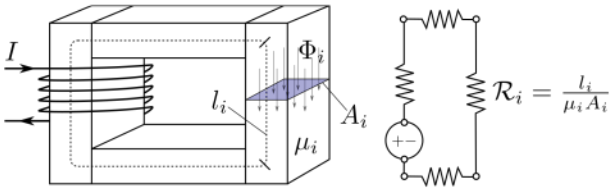

Fig. 2. Simple magnetic circuit with its equivalent model on the right. Flux Φ_i and flux density are related by the perpendicular area: $B_i = \Phi_i / A_i$

of the *magnetic field strength* $\boldsymbol{H}$ over a contour C yields the total current in the body enclosed by that contour and from *Gauss' law* follows that the integral of the *magnetic flux density* $\boldsymbol{B}$ over the bodies surface S must equal to zero:

$$\oint_C \boldsymbol{H} \cdot d\boldsymbol{l} = I_{tot}, \qquad \oint_S \boldsymbol{B} \cdot d\boldsymbol{s} = 0$$

By assuming the field lines of $\boldsymbol{H}$ and $\boldsymbol{B}$ in parallel to the integration paths, lumped parameter models can be deduced when the cross-section area is constant, like in Fig. 2. Magnetic flux density and magnetic field strength of each element i are related by the *permeability*[2] μ_i such that $B_i = \mu_i H_i$. *Kirchhoff's* laws apply from here on and circuits can be computed by solving the underlying system of equations, once that all flux paths are modeled by their equivalent *reluctances* $\mathcal{R}_i$ in the system. One difficulty by employing the MEC method are geometric changes when the modelled machine moves, that a global model needs to account for. This work follows the analytical model that was derived in [14] with geometric parameters depicted on top of Fig. 3. The circular shape of the motor is considered being the depicted unwind analog and flux paths shown at the bottom of Fig. 3 are modelled inside the computational domain 2τ. Via conditional statements, the modeling formulas ensure validity for motor positions inside the *half-pitch* $\tau/2$. Flux paths through air only have a geometric dependence, whereas the reluctance (or permeability) of (soft) magnetic material is a function of flux density itself and therefore depends on the field strength inside the material. This requires to solve a non-linear system of equations. Once the flux in the air gap ϕ_g is deduced from the model, the induced voltage per winding n_w and per speed ω_m (also named *specific back-EMF*) is obtained with

$$sbEMF(x) = \frac{d\phi_g}{dx} \cdot n_p \tag{1}$$

depending on motor position x and the pole number n_p of the motor.

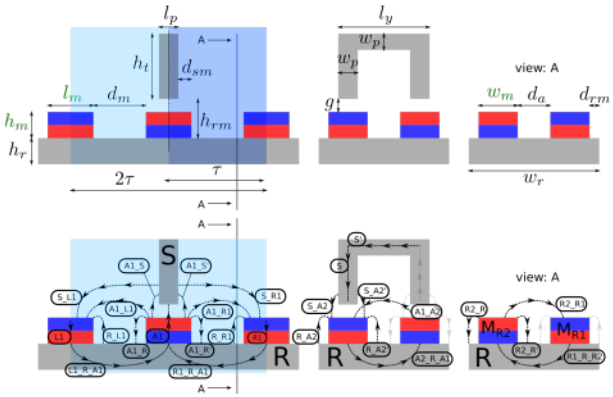

Fig. 3. Transverse Flux Machine in unwind depiction with geometric parameters and modeled flux paths - adapted from [14]

3. MOTOR DESIGN PROCEDURE

A suitable approach to assemble and solve the non-linear MEC was found by employing `OpenModelica` along with the editor `OMEdit` that supplies material libraries and related saturation models. Computation of reluctances and overall control of the procedure is carried out in `Julia`, allowing for high modeling flexibility under high speed in computations. The MEC related to the reluctances shown in Fig. 3 is provided in Fig. 4

3.1 Genetic Algorithm

In order to obtain an efficient motor geometry for the purpose of the desired drive, a genetic algorithm is used to sweep through a sufficient big parameter space of designs. The sequence can be seen in Alg. 1 and requires geometric and performance values as input - see Sec. 4.

[2] Expressed by the permeability of vacuum μ_0 and the relative permeability of the material: $\mu_i = \mu_0 \mu_{ri}$

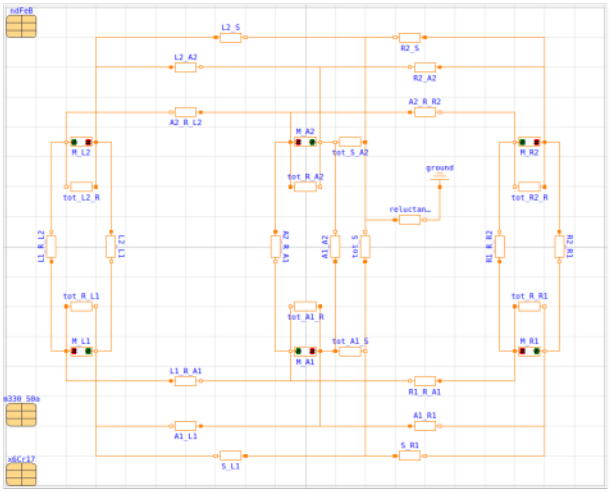

Fig. 4. Magnetic Equivalent Circuit of the TFM in `OMEdit` - naming matches with Fig. 3

Algorithm 1 Adapted genetic algorithm

```
1:  function GeneticOptimization(design0, population, var, red, w, ω_m, I, U)
2:      for i=1 : population do
3:          design[i] = GeometryVariation(design0, var[1])
4:      end for
5:      while population > survivors do
6:          for i=1 : population do
7:              sbEMF[i] = SpecificBackEMF(design[i])
8:              fitness[i] = w[1,1]·RootMeanSquare(sbEMF[i]) + w[1,2]/EstimateMass(design[i])
9:          end for
10:         design = SortBy(fitness)
11:         design = design[1 : red[1]]
12:         population = population·red[1]
13:         for i=1 : population do
14:             design[i] = DeduceCoilGeometry(design[i], sbEMF[i], ω_m, U)
15:             R[i] = CoilResistance(design[i])
16:             fitness[i] = w[2,1]·/(I^2·R[i]) + w[2,2]/EstimateMass(design[i])
17:         end for
18:         design = SortBy(fitness)
19:         design = design[1 : red[2]]
20:         population = population·red[2]
21:         for i=population/2 : population do
22:             design[i] = GeometryVariation(design[i], var[2])
23:         end for
24:     end while
25:     return geometry
26: end function
```

The function `GeometryVariation()` alters - with exception of the magnets geometry - all parameters with dependence on the randomly changed parameters n_p, d_i, h_r, l_p, g, w_p, h_t, l_y and d_{rm}. This is done to avoid geometric unfeasible designs in the parameter sweep. After creating an initial population (Alg. 1, l. 3) the algorithm enters into a while-loop until `population` is reduced to a maximal size `survivors`. This is achieved by three subsequent steps:

1. Reduction of the population by means of a fitness value involving the specific back-EMF of the motor and its mass without coil (Alg. 1, l. 6-12).
2. Further reduction of the remaining designs by involving the coil heat losses and the motors masses with coil (Alg. 1, l. 13-19).
3. Altering the second half of designs (sorted by fitness) by a random process.

This procedure is tailored to favour designs that meet a required operating voltage and to treat the occurring coil resistance only in a second step. In Alg. 1, l. 15 the magnetic saturation of the stator core is additionally checked and the coil inductance could also be involved when higher rotation speeds are of interest. Motor masses are computed from the weights of coil, stators, magnets and rotor and does not involve constructive elements.

4. RESULTS AND DISCUSSION

Alg. 1 has been performed for different (commercially available) magnet sizes, whereas results obtained from the ones specified in Tab. 4are shown in Fig. 5 and 6. In both cases, the design set was reduced from 10^4 to 2. In both figures a reduction in mass and coil resistance can be observed over the different seasons. This happens at the cost of reduced inductance in both cases and restrictions arise from the feasibility of designs (indicated by grey line). For the bigger magnets, a tendency towards motors with higher $sbEMF$, that are heavier than their predecessors, can be seen over the different seasons. For the application in question, lightweight motors prevail and the finally designed drive of Fig. 1 resulted from the simulations with small magnets. In Fig. 7, the flux linkage over the normalised motor pitch of initial and final design can be seen, showing similar curve shapes. However, the estimated mass of the final design is drastically reduced from 0.41 kg to 0.095 kg. For a first design phase of

Table 1. Specified parameters to perform Alg. 1, geometric variables depicted in Fig. 3 with d_i as inner diameter

`population`	10^4
`var`	[0.5*ones(9), 0.1*ones(9)] - parameter variances
`red`	[0.4, 0.75] - reduction ratios
`w`	[1 5e-4; 1 3] - fitness function weights
ω_m	400 rpm
`I`	1 A
`U`	12 V
`design0`: "small magnets"	$l_m = 4$ mm, $w_m = 4$ mm, $h_m = 1.5$mm, $n_p = 15$, $d_i = 60$ mm, $h_r = 5$ mm, $h_t = 15$ mm, $g = 1$ mm, $w_p = 3$ mm, $l_p = 3$ mm, $l_y = 15$ mm
`design0`: "big magnets"	$l_m = 10$ mm, $w_m = 10$ mm, $h_m = 5$mm, $n_p = 9$, $d_i = 65$ mm, $h_r = 5$ mm, $h_t = 15$ mm $g = 1.5$ mm, $w_p = 5$ mm, $l_p = 10$ mm, $l_y = 25$ mm

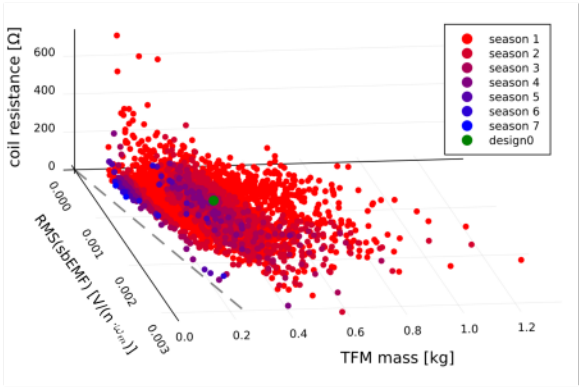

Fig. 5. Data points of resulting designs from simulation with "small magnets"

TFMs, we showed a useful procedure to obtain motor geometries that can serve for constructing a TFM or starting more elaborated simulations, like FEM. Despite the use-

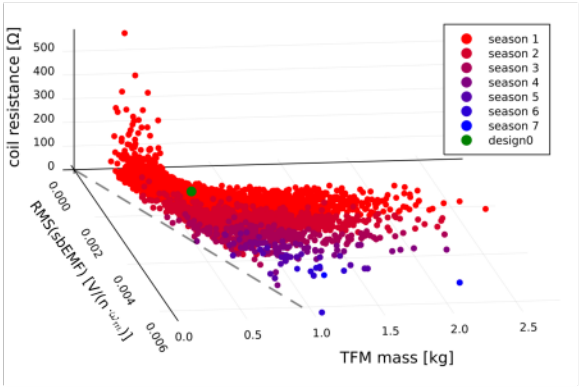

Fig. 6. Data points of resulting designs from simulation with "big magnets"

fulness of the approach, we are aware that the modeling by analytical functions can only cover a certain parameter range and brings some inaccuracy with it, as can e.g. be seen by the jagged flux curves of Fig. 7. Accordingly, the presented algorithm is at risk to optimise rather for designs that can be well modeled than designs of best performance. Therefore, more research is required to validate the here presented outcomes. We however believe that our approach can serve to bring direct drives faster into their desired applications.

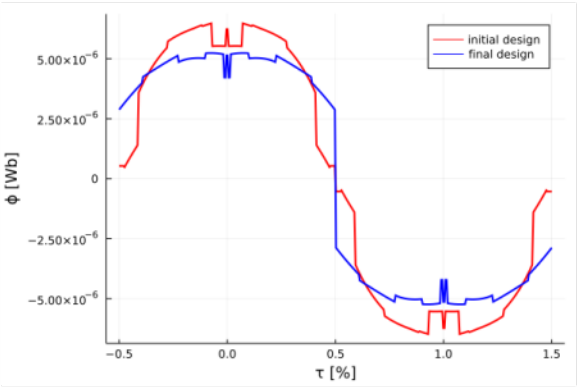

Fig. 7. Simulation results of the magnetic flux linkage of the initial and final design with "small magnets". Computations range from $0 - 0.5\,\tau$ and other regions are mirrored values.

ACKNOWLEDGEMENT

Funded by the Deutsche Forschungsgemeinschaft (DFG, German Research Foundation) - 404971005.

REFERENCES

[1] H. Asada and T. Kanade, "Design of Direct-Drive Mechanical Arms", *Journal of Vibration, Stress, and Reliability in Design*, vol. 105, pp. 312-316, 1983

[2] G.C. Kennedy and J.K. Holt, "Developing a High Efficiency Means of Propulsion for Underwater Vehicles", *Proceedings of Southcon '95, IEEE*, pp. 352-356, 1995

[3] E.P. Furlani, "Permanent Magnet and Electromechanical Devices", *Elsevier*, 2001

[4] A. Babazadeh and N. Parspour and A. Hanifi, "Transverse Flux Machine for Direct Drive Robots: Modelling and Analysis", *Conference on Robotics, Automation and Mechatronics*, pp. 376-380, 2004

[5] M. Kowol and M. Łukaniszyn and K.J. Latawiec, "Optimization of a Transverse Flux Motor Using an Evolutionary Algorithm", *IFAC Proceedings Volumes*, vol. 42, pp. 71-76, 2009

[6] S. Seok and A. Wang and D. Otten and S. Kim, "Actuator Design for High Force Proprioceptive Control in Fast Legged Locomotion", *International Conference on Intelligent Robots and Systems, IEEE*, pp. 1970-1975, 2012

[7] R. D. Christ and R.L. Wernli, "The ROV Manual - A User Guide for Remotely Operated Vehicles", *ELSEVIER*, Chapter 6, 2014

[8] Y. Tang and J.J.H. Paulides and E.A. Lomonova, "Analytical Modeling of Flux-Switching In-Wheel Motor Using Variable Magnetic Equivalent Circuits", *ISRN Automotive Engineering*, pp. 1-10, 2014

[9] P. Kampmann and F. Kirchner, "Towards a fine-manipulation system with tactile feedback for deep-sea environments", *Robotics and Autonomous Systems*, vol. 65, pp. 115-121, 2015

[10] M.F.J. Kremers, "Analytical design of a transverse flux machine", Eindhoven: Technische Universiteit Eindhoven, 2016

[11] K. M. Lynch and F. C. Park, "Modern Robotics - Mechanics, Planning, and Control", *Cambridge University Press*, Chapter 8.9.2, 2017

[12] T. Husain and I. Hasan and Y. Sozer and I. Husain and E. Muljadi, "A Comprehensive Review of Permanent Magnet Transverse Flux Machines for Direct Drive Applications", *IEEE*, pp. 1255-1262, 2017

[13] J. Zhu and C. White and D.K. Wainwright and V. Di Santo and G.V. Lauder and H. Bart-Smith, "Tuna robotics: A high-frequency experimental platform exploring the performance space of swimming fishes", *Science Robotics*, vol. 4, pp. 1-12

[14] A.A. Pourmoosa and M. Mirsalim and A. Mahmoudi and S. Vaez-Zadeh, "Analytical model based on magnetic equivalent circuit for transverse-flux permanent-magnet machines", *Int Trans Electr Energ Syst.*, vol. 30, 2020